CBIR of Spine X-ray Images on Inter-vertebral Disc Space and Shape Profiles

Yuchou Chang [a] , Sameer Antani [b] , D.J. Lee [a] , Kent Gledhill[c], L.Rodney Long [b] , Paul Christensen[a]

[a] *Department of Electrical and Computer Eng., Brigham Young University, Provo, UT*

yuchou.chang@gmail.com, djlee@ee.byu.edu, paulchst@gmail.com

[b]National Library of Medicine, National Institutes of Health, Bethesda, Maryland

antani@nlm.nih.gov, long@nlm.nih.gov

[c]*Utah Valley Regional Medical Center, Provo, Utah*

kmgtmg@comcast.net

Abstract

There is very limited research published in the literature that applies content-based image retrieval (CBIR) techniques to retrieval of digitized spine X-ray images using a combination of inter-vertebral disc space and shape profiles. We present a novel technique to retrieve vertebra pairs that exhibit a specified disc space narrowing (DSN) and inter-vertebral disc shape profile. DSN is characterized using spatial and geometrical features between two adjacent vertebrae. Initial retrieval results are clustered and used to construct a voting committee to retrieve vertebra pairs with the highest DSN similarity. Experimental results show that the proposed algorithm is a promising approach for disc space-based spine X-ray image retrieval. The overall retrieval accuracy validated by a radiologist is 82.25%.

1. Introduction

Content-Based Image Retrieval (CBIR) has been studied since the 1990s. These techniques have been used for searching images in digital libraries, on the World Wide Web, and other applications such as trademark search [1]. Research on medical image retrieval, however, has been fairly recent [2-7]. These efforts can be broadly categorized into two themes: (i) retrieval of biomedical images from a heterogeneous collection (images of different anatomy, modality, and detail) with little importance given to localized pathology, and (ii) retrieval of images from a homogenous collection (images of single modality, anatomy, and detail) with particular focus on the localized pathology. Our previous research is of the latter category [8].

Osteoarthritis affects a significant portion of the elderly population in the United States [9]. Osteophytes, disc space narrowing (DSN), subluxation and spondylolisthesis on the spine are typical radiographic hallmarks characterizing this condition. The ability to retrieve images of the spine on these conditions would be very valuable to researchers of osteoarthritis and musculoskeletal diseases, educators, and radiologists. Reference images are often used to determine the extent of DSN reinforcing the need, for visual retrieval of typical cases.

The Lister Hill National Center for Biomedical Communications, an intramural R&D division of the National Library of Medicine (NLM) at the National Institutes of Health, maintains an archive of digitized spine X-rays collected from the second National Health and Nutrition Examination Surveys (NHANES II) [10] which could be used for such a reference collection. Very limited published research is devoted to CBIR of such images on DSN and inter-vertebral disc shape profiles. Figure 1(a) shows two adjacent vertebrae outlined on a lumbar spine X-ray.

Manually finding reference images from a large image database is a tedious and error prone process. An automatic CBIR system can significantly alleviate the problem of retrieving relevant images with specified DSN. A prior study [11] proposes use of four scale-invariant, distance transform-based features to characterize spacing between adjacent vertebrae. *K*-means clustering and self-organizing map (SOM) were used to classify inter-vertebral disc space and assigned it a degree of DSN severity with an overall accuracy of 82.1%. A shortcoming of this approach for shape-based CBIR was the lack of disc shape profiles. This can have an adverse impact when querying by DSN severity alone is insufficient.

Vertebral shape is valuable in expressing the spine conditions described earlier. As seen in the sagittal

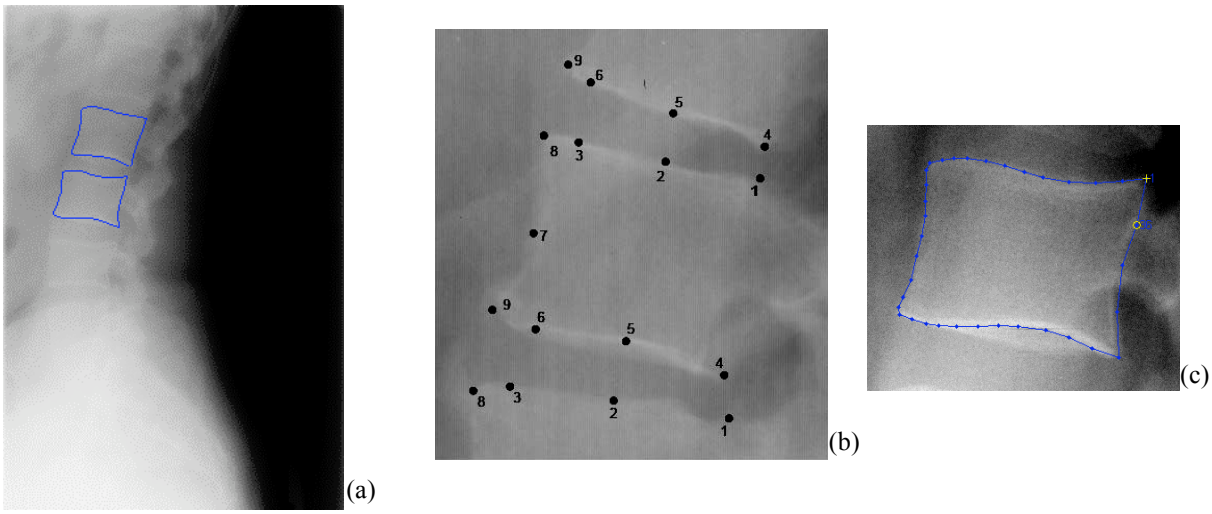

Figure 1. (a) Spine X-ray image with the superimposed shape contours on two adjacent vertebrae, (b) 9-point model, and (c) 36-point contour.

view, the inferior and superior edges of vertebrae adjacent to the disc can serve as the disc shape profile. Experienced radiologists use several criteria when evaluating DSN similarity between a candidate case and references from an atlas, for example. These criteria include the top to bottom size of the intervertebral gap, the length of the gap, and its configuration, i.e., whether there are spurs, concavities, convexities, irregularities, etc. Many of these disc space characteristics can be computed from disc shape profiles. In this paper, we present two approaches that combine disc shape profile with computed inter-vertebral disc space features, one of which uses voting consensus for finding similar images. In addressing this important problem, this effort makes advances the state of the art in CBIR taking advantage of clustering ensemble based machine learning methods [1, 12-15].

The proposed algorithm and DSN similarity measures are discussed in Section 2. Section 3 introduces the proposed voting consensus mechanism. Experimental results and analysis are presented in Section 4. Conclusions and future directions are described in Section 5.

2. Methods

X-ray images in the database for this study are pre-segmented using semi-supervised methods and the resulting 9-point and 36-point contour shapes are validated by a board certified radiologist. Examples of these contours are shown in Figures 1(b) and 1(c). Figure 1(b) shows the 9-point model commonly used by radiologists. The left side (Points 8-7-9) of the vertebra is the anterior edge and the right side (Points 1-4) is the posterior edge. Figure 1(c) shows a vertebra contour represented by 36 points. More points are used for the anterior side because it has more anatomical importance than the posterior side. In cervical and lumbar images, we use up to 4 disc inter-vertebral spaces between C3-C7 and L1-L5 vertebrae, respectively.

In the sagittal view, a 9-point vertebral contour includes the superior and inferior "corners" on both anterior and posterior sides of the vertebra (Points 1, 8, 4, and 9). These four corners are treated as salient points to guide the calculations of spatial and geometrical features. The approximate centroid of the vertebra for feature extraction is calculated as shown in Equation. (1), where, (x_c,y_c) are the coordinates of the centroid, and (x_i,y_i) are the coordinates of four corner points.

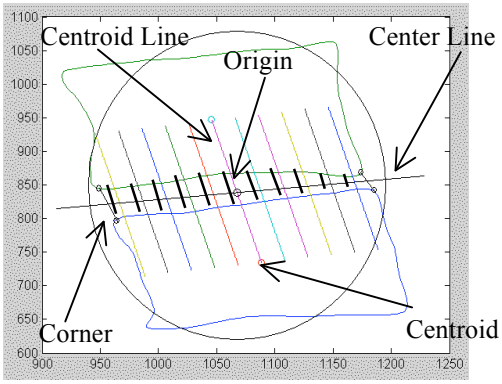

Figure 2. Centroids of two adjacent vertebrae, centroid line that connects centroids, lines parallel to the centroid line at a fixed interval, anterior and posterior corners, and the center line that separates the vertebrae.

$$(x_c, y_c) = \frac{1}{4}\sum_{i=1}^{4}(x_i, y_i) \quad (1)$$

As shown in Figure 2, connecting the two centroids of the upper and lower vertebrae, a line segment called centroid line is formed and is divided into three segments. These sections include two segments in the interior of these vertebrae from the centroids to the edges of vertebrae and the middle segment in the inter-vertebral area (darkened line). The length of the segment in the inter-vertebral area is treated as one of many distance measures of DSN. Additionally, since the inter-vertebral disc shape profile, defined as the pair of contour edge segments between the respective inferior and superior corners of these adjacent vertebrae, are not a straight line, distance measure along the centroid line alone cannot typify the DSN. Ten line segments parallel to the centroid line that equally divide the width of the vertebra are generated. From these 11 parallel lines resulting inter-vertebral disc space distances are used to compute their mean and standard deviation and are used to represent the degree of DSN.

The asymmetry in the disc space is computed as *Skewness* using polar coordinates that have previously been applied in shape representation and analysis [16-17]. It is computed as the difference between the inter-vertebral distance between anterior and posterior "corners" using the 9-point model. Two short line segments can be formed by connecting the two anterior corners and the two posterior corners. The center line, also shown in Figure 2, can then be formed by connecting the mid points of these two short line segments. This center line is treated as the X-axis of a polar coordinate system. Furthermore, the intersection of this X-axis and the centroid line is used as the origin of the coordinate system. Based on this origin and the X-axis, the skewness of DSN is calculated as:

$$Skewness = \left|(\theta_{rt} + \theta_{rb})\right| - \left|(\theta_{lt} + \theta_{lb})\right| \quad (2)$$

, where

$$\theta = \sin^{-1}\left(\frac{\text{Distance to the x - axis}}{\text{Distance to the Origin}}\right), \quad (3)$$

In Equation (2), θ_{rt} is the angular measurement between the posterior-inferior corner of the upper vertebra and the origin. Similarly, θ_{rb} is the angular measurement between the posterior-superior corner of the lower vertebra and the origin. Correspondingly, θ_{lt} and θ_{lb} can be computed similarly. All angular measurements are calculated using Equation (3). The *Skewness* measure is positive when the short line segment on the right is longer than the one on the left. Otherwise, the *Skewness* is negative.

These three spatial features, the mean and standard deviation of 11 parallel line segments and and *Skewness* are used to characterize the spatial and geometrical aspects of the inter-vertebral disc space and can subsequently be used in DSN-based retrieval.

In order to more accurately retrieve vertebra pairs with similar DSN characteristics, inter-vertebral disc shape profile is also included. This shape profile is the set of shapes described earlier as the vertebral contour between two inferior corners and two superior corners of respective adjacent vertebrae. To compute shape profile similarity, we use the Procrustes distance measure [18]. This distance measure requires and equal number of points on the shapes under comparison. We interpolate each segment in the shape profile to obtain 115 points between the two corners that form the candidate shape profile.

3. Voting consensus

Generally, CBIR system retrieves images by comparing the query image against images in the database using similarity measures. Voting consensus has shown success in clustering ensemble [12], object classification [13], and information extraction [14]. In [15], authors used a clustering algorithm to retrieve clusters of images that are in the vicinity of the query image. These clusters can be deemed as semantic groups. This paper presents a voting consensus mechanism to achieve a similar task. Using voting consensus for a query inter-vertebral disc, Q_0, a set of M discs with similarly expressed (using shape profiles) and with indicated proximity (using DSN measures) can be retrieved. In order to associate every retrieved image to its semantic category, K-means clustering [19] is used to partition these M retrieved images into K ($K \leq M$) clusters.

After the partitioning process is completed, a pre-selected number of discs, N, in the cluster that contains the original query disc, Q_0, are chosen as new queries, (Q_1, Q_2,$\cdots$, Q_N). Using these N new queries and the spatial and geometrical features as the similarity measures, M images most similar to each of these N new queries can, then, be retrieved.

This whole initial retrieval process provides a total of N+1 sets of retrieval results (the original query and N new queries) that are used as the members of the voting committee. Each of these sets of retrieval result consists of M discs most similar to its query. Furthermore, profile similarity measured using the Procrustes distance is also used to retrieve M discs to form another set of retrieval result using the original query Q_0. Adding this set of retrieval result to the voting committee results in a total of N+2 voting

committee members. Each of the M images in their own set of retrieval result has its position on the similarity ranking list, where, the top ranked image is most similar to the query image and the image ranked at position M is least similar to the query image. The voting process is performed according to the procedure below.

(1) For each image I_i (where i represents the position of image I on the ranked response list to the original query Q_0), its vote from committee member 0 is calculated as $B_{i0}=M-(i-1)$, $i=1,2,\cdots,M$.

(2) Image I_i also receives a vote from committee member j that is calculated as $B_{ij}=M-(|P_0-P_i|)$, $i=1,2,\cdots,M$, $j=1,2,\cdots,N$. P_0 is the position of the original query Q_0 on the ranked response list to query Q_j (committee member j). P_i is the position of image I_i on the ranked response list to the original query Q_0 (committee member 0). The vote $B_{ij}=0$ if Q_0 or I_i is not ranked as the top M in committee member j.

(3) Repeat (2) for all N sets of initial retrieval result.

(4) Image I_i also receives a vote from the last committee member that is generated by using profile similarity and the original query Q_0. The vote is calculated as $B_{i(N+1)}= M-(i-1)$, $i=1,2,\cdots,M$. $B_{i(N+1)}=0$ if I_i is not ranked as the top M in the last committee member.

(5) Calculate I_i's total vote from N+2 committee members from Steps 1, 2, and 4 as $B_i = \sum_{j=0}^{N+1} B_{ij}$.

(6) The final retrieval result can be obtained by sorting B_i.

This final retrieval result is then reverse ordered set of unique discs from those with most votes to those with the least. This list may be further reduced for application purposes. Figure 3 shows the framework of the proposed algorithm.

4. Experimental results

A set of 801 cervical and 972 lumbar vertebral outlines (shapes) segmented from a total of 400 digitized spine X-ray images was used for performance evaluation. Ten disc pairs of both cervical and lumbar shapes were selected randomly as queries. From the set of cervical vertebrae outlines, pairs of adjacent vertebrae were used to identify discs. Three discs from the C3-C4 pair, 2 discs from the C4-C5 pair, 3 discs from the C5-C6 pair, and 2 discs from the C6-C7 vertebrae pair were selected as queries. Five of these query shapes had osteophytes. One of them had slight osteophytes and two were moderate and two were severe. Similarly, from the set of lumbar vertebrae outlines, 3 disc pairs of L1-L2, 2 disc pairs of L2-L3, 3 disc pairs of L3-L4, and 2 disc pairs of L4-L5 were selected as queries. Half of them had osteophytes. Two of them had slight osteophytes and one was moderate and two were severe. The proposed voting consensus algorithm was compared with direct retrieval based on disc space measurements without a voting committee.

Twenty queries comprising of: 10 discs from pairs of cervical and lumbar vertebrae outlines, respectively, were used in the evaluation. The set of retrieved vertebrae pairs were limited to the top 20 pairs for each query generating a result set of 200 vertebrae pairs for cervical and lumbar vertebrae queries, respectively.

Figures 4 to 7 are screenshots showing examples of retrieval results. Figures 4 and 6 show the top 20 retrievals using the proposed algorithm for cervical and

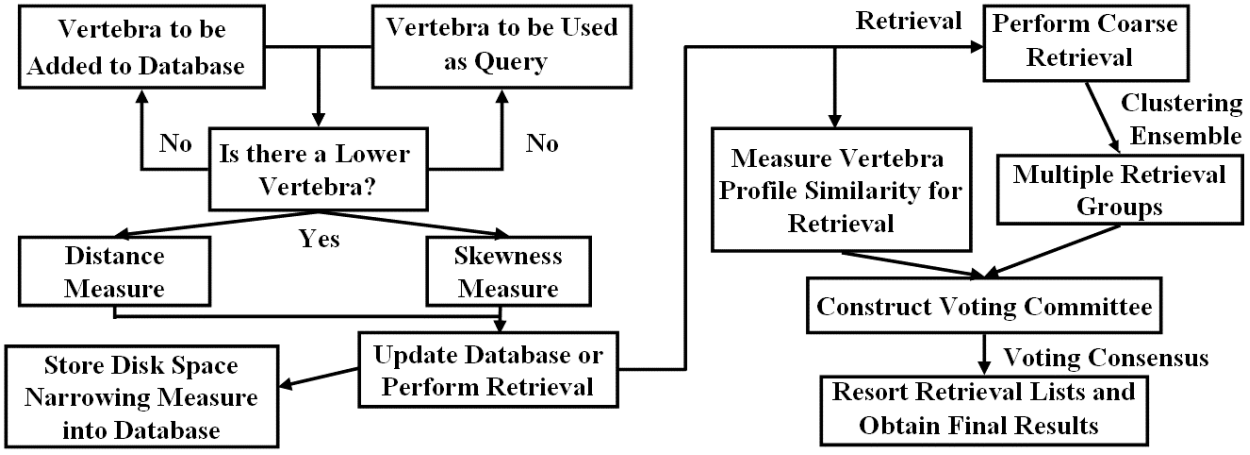

Figure 3. Algorithm framework.

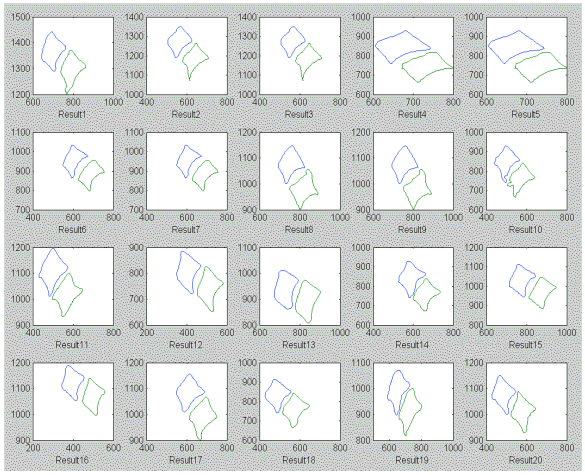

Figure 4. Retrieval result of cervical disc pairs using the proposed algorithm.

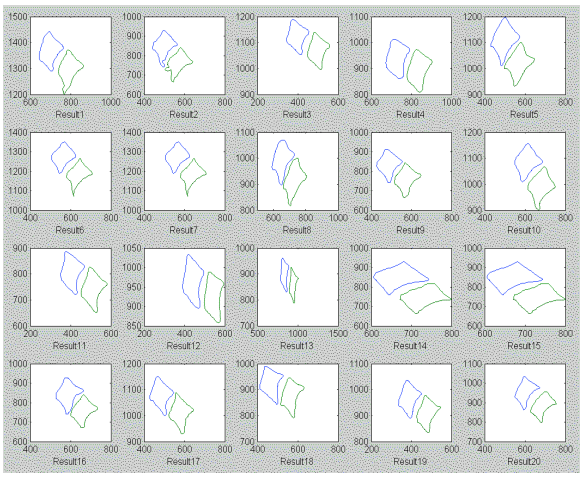

Figure 5. Retrieval result of cervical disc pairs without voting committee.

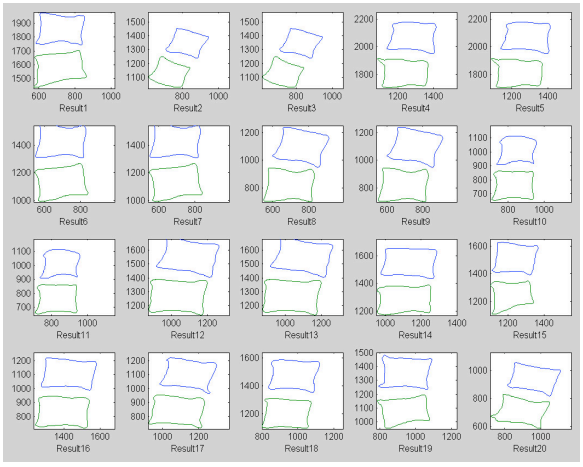

Figure 6. Retrieval result of lumbar disc pairs using the proposed algorithm.

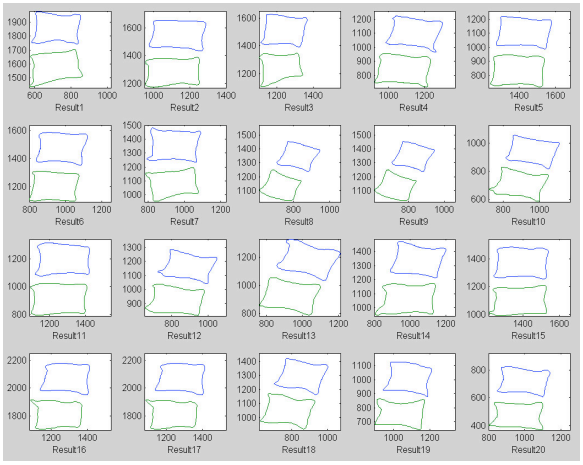

Figure 7. Retrieval result of lumbar disc pairs without voting committee.

lumbar disc pairs, respectively. Figures 5 and 7 show the top 20 retrievals using direct retrieval without voting committee. In viewing these images, a layperson, can verify the method appears to perform as desired. It is necessary, however, for trained eyes to evaluate its performance.

Table 1 shows the retrieval results that were validated by a board certified radiologist specializing in diseases of the spine. Without the use of voting consensus mechanism, 123 cervical pairs of 200 retrieved (61.5%) and 185 of 200 (92.5%) lumbar pairs were validated as relevant, respectively. The overall retrieval accuracy was 77% (308/400). In contrast, with the proposed voting consensus mechanism, 140 of 200 (70%) retrieved cervical pairs and 189 of 200 (94.5%) retrieved lumbar pairs were validated as relevant, respectively. The overall retrieval accuracy of the proposed algorithm was 82.25%, which showed an improvement over the direct retrieval without voting consensus.

TABLE 1: Retrieval results with and without voting consensus mechanism.

	Cervical	Lumbar	Percentage
Without Voting	123	185	77%
With Voting	140	189	82.25%

5. Conclusion

This paper presents a novel approach for content-based retrieval of vertebra pairs using spatial and geometrical constraints applied to inter-vertebral disc space and using both the 9-point and 36-point vertebral shape profiles. The mean and standard deviation of disc space distances and skewness measures are used as the spatial and geometrical properties of DSN. A voting committee is constructed based on the retrieval

results using these properties as well as the vertebral shape profile similarity which improves the retrieval accuracy by 5%. This is significant when applied for specific queries on localized pathology expressed in large image collections. It is also interesting to note that the overall retrieval accuracy remains about the same as the earlier approach for DSN classification while including the use of shape profiles, thus enabling its use in CBIR applications.

6. Acknowledgements

This work research was supported in part by the National Library of Medicine (NLM) under Grant contract HHSN276200700335P and intramural research funds of the Lister Hill National Center for Biomedical Communications, the National Library of Medicine (NLM), and the National Institutes of Health (NIH).

7. References

[1] Smeulders, A.W.M., Worring, M., Santini, S., Gupta, A., Jain, R., Content-Based Image Retrieval at the End of The Early Years, IEEE Transactions on Pattern Analysis and Machine Intelligence, vol.22, issue.12, pp.1349-1380, 2000.

[2] El-Naqa, I., Yongyi Yang, Y. Galatsanos, N.P., Nishikawa, R.M., Wernick, M.N. A Similarity Learning Approach to Content-Based Image Retrieval: Application to Digital Mammography, IEEE Transactions on Medical Imaging, vol.23, issue.10, pp.1233-1244, 2004.

[3] Kim, J., Cai, W., Feng, D., Wu, H., A New Way for Multidimensional Medical Data Management: Volume of Interest (VOI)-Based Retrieval of Medical Images With Visual and Functional Features, IEEE Transactions on Information Technology in Biomedicine, vol.10, issue.3, pp.598-607, 2006.

[4] Mojsilovic, A., Gomes, J., Semantic Based Categorization, Browsing and Retrieval in Medical Image Databases, International Conference on Image Processing, vol.3, 2002.

[5] Greenspan, H., Pinhas, A.T., Medical Image Categorization and Retrieval for PACS Using the GMM-KL Framework, IEEE Transactions on Information Technology in Biomedicine, vol.11, issue.2, pp.190-202, 2007.

[6] Lehmann, T.M., Wein, B.B., Keysers, D., Kohnen, M., Schubert, H., A Monohierarchical Multiaxial Classification Code for Medical Images in Content-Based Retrieval, IEEE International Symposium on Biomedical Imaging, pp.313-316, 2002.

[7] Liu, W., Tong, Q.Y., Medical Image Retrieval using Salient Point Detector, IEEE-EMBS 27th Annual International Conference of the Engineering in Medicine and Biology Society, pp.6352-6355, 2005.

[8] X.Q. Xu, D.J. Lee, S.K. Antani, and L.R. Long, "A Spine X-ray Image Retrieval System Using Partial Shape Matching," IEEE Transactions on Information Technology in Biomedicine, vol. 12/1, p. 100-108, January 2008.

[9] Fact Sheet: Osteoarthritis. American College of Rheumatology, Atlanta, Georgia, 1994.

[10] Long, L.R., Thoma, G.R., Image Query and Indexing for Digital X-rays, SPIE Conference on Storage and Retrieval for Image and Video Databases VII, vol. 3656, pp.12-21, 1999.

[11] Chamarthy, P., Stanley, R.J., Cizek, G., Long, Rodney., Antani, S., Thoma, G., Image Analysis Techniques for Characterizing Disc Space Narrowing in Cervical Vertebrae Interface, Computerized medical Imaging and Graphics, vol.28, pp.39-50, 2004.

[12] Avad, H.G., and Kamel, M.S., Cumulative Voting Consensus Method for Partitions with Variable Number of Clusters, IEEE Transactions on Pattern Analysis and Machine Intelligence, vol.30, no.1, pp.160-173, 2008.

[13] Berg. T.L., and Forsyth, D.A., Animal On the Web, IEEE International Conference on Computer Vision and Pattern Recognition, vol.2, pp1463-1470, 2006.

[14] Sigletos, G., Paliouras, G., Spyropoulos, C., and Hatzopoulos, M., Combining Information Extraction Systems Using Voting and Stacked Generalization, Journal of Machine Learning Research, vol.6, pp.1751-1782, 2005.

[15] Chen, Y., Wang, J.Z., and Krovetz, R., CLUE: Clustering-Based Retrieval of Image by Unsupervised Learning, IEEE Transactions on Image Processing, vol.14, no.8, pp.1187-1201, 2005.

[16] Baloch, S.H., and Krim, H., Flexible Skew-Symmetric Shape Model for Shape Representation, Classification, and Sampling, IEEE Transaction on Image Processing, vol.16, no.2, 2007.

[17] Srivastava, A., Joshi, S.H., Mio, W., and Liu, X., Statistical Shape Analysis: Clustering, Learning, and Testing, IEEE Transactions on Pattern Analysis and Machine Intelligence, vol.27, no.4, 2005.

[18] Seber, G. A. F., Multivariate Observations, Wiley, 1984.

[19] MacQueen, J.B., Some Methods for Classification and Analysis of Multivariate Observations, Proceedings of 5-th Berkeley Symposium on Mathematical Statistics and Probability, Berkeley, University of California Press, vol.1, pp.281-297, 1967.